Developmental Biology 531 (2026) 19–29

Contents lists available at ScienceDirect

Developmental Biology

journal homepage: www.elsevier.com/locate/developmentalbiology

Original research article

A morphometric characterization of early CHICK embryo elongation

A.C. Maia-Fernandes [a,b], T. Pais de Azevedo [a,b,c,1], N. Borralho-Martins [a,b,1], S. Ramalhete [b], G.G. Martins [c,d], I. Palmeirim [a,b,e], I. Duarte [b,f], A. Marreiros [a,b], P.J. Martel [f,g], R.P. Andrade [a,b,e,*]

[a] ABC-RI, Algarve Biomedical Center Research Institute, Faro, Portugal
[b] Faculdade de Medicina e Ciências Biomédicas (FMCB), Universidade Do Algarve, Campus de Gambelas, 8005-139, Faro, Portugal
[c] Faculdade de Ciências, Universidade de Lisboa, 1749-016, Lisbon, Portugal
[d] Gulbenkian Institute for Molecular Medicine (GIMM), Portugal
[e] Champalimaud Research Program, Champalimaud Center for the Unknown, Lisbon, Portugal
[f] CINTESIS@RISE, Universidade Do Algarve, Faro, Portugal
[g] Faculdade de Ciências e Tecnologia (FCT), Universidade Do Algarve, Campus de Gambelas, 8005-139, Faro, Portugal

ARTICLE INFO

Keywords:
Chicken embryo
Length measurements
Morphometric tool
Time-lapse imaging

ABSTRACT

The chicken embryo has long been a pivotal model system to understand the cellular and molecular mechanisms driving amniote embryo development. Its easy access for *in vivo* experimentation, together with the development of *ex ovo* culture techniques, has made it a choice model system for elaborate experimental manipulations. Temporal progression of chick embryo development is classically categorized using the Hamburger and Hamilton staging system (Hamburger, V., & Hamilton, 1951). However, this offers limited temporal resolution when comparing embryos within the same developmental stage and may further be hindered by experimental conditions that directly impact the morphological structures used for stage identification. Here, we performed time-lapse imaging of early chick embryonic stages HH4 to HH10 and obtained quantitative elongation data of multiple embryonic portions, yielding two valuable and freely accessible data resources for the chick research community. We identified length measurements capable of describing developmental time, thus enabling the alignment of independent embryos with temporal resolution. Notably, the head-fold (C-HF) showed a strong time correlation, even though it elongates above the primary embryonic axis. A morphometric characterization of HH stages further showed that C-HF length can discriminate HH stages of development, albeit with limited resolution. Finally, we present **ChEEQ**: **Ch**icken **E**mbryo **E**longation **Q**uantification (https://colab.research.google.com/github/EmbryoClock/ChickElong/blob/main/ChEEQ/ChEEQ.ipynb), a new morphometric tool describing HH4-HH10 embryo elongation, that allows the comparison of user-input data with our reference dataset and is capable of inferring quantitative alterations to embryo developmental time using length measurements alone. Together, these resources open new avenues for investigating vertebrate embryo elongation and quantitatively assessing the effects of experimental interventions on development.

1. Introduction

The chicken embryo is an extraordinary model system. With over 2000 years of history, it remains a valuable embryo model, with contributions that span many fields of knowledge (Stern, 2005). During early developmental stages, the chick embryo shares a striking resemblance to the human embryo, namely during gastrulation and embryo body segmentation, while lending itself to direct *in vivo* visualization and experimentation (Stern, 2005). Elongation of the chicken embryo along the anterior-posterior (AP) axis is very dynamic in both time and

This article is part of a special issue entitled: Avian model systems published in Developmental Biology.

* Corresponding author. ABC-RI, Algarve Biomedical Center Research Institute Campus de Gambelas, Ed2 - Ala Norte Universidade do Algarve 8005-139 Faro Portugal.

E-mail addresses: ac.maia.fernandes@gmail.com (A.C. Maia-Fernandes), tompaisazevedo@gmail.com (T. Pais de Azevedo), nisiabmartins@gmail.com (N. Borralho-Martins), saravramalhete@gmail.com (S. Ramalhete), gaby@igc.gulbenkian.pt (G.G. Martins), ipalmeirim@gmail.com (I. Palmeirim), giduarte@ualg.pt (I. Duarte), ammarreiros@ualg.pt (A. Marreiros), pmartel@ualg.pt (P.J. Martel), rgandrade@ualg.pt (R.P. Andrade).

[1] equal contribution.

https://doi.org/10.1016/j.ydbio.2025.12.022
Received 30 October 2024; Received in revised form 17 November 2025; Accepted 25 December 2025
Available online 2 January 2026

space. The embryonic AP axis is first established by the primitive streak (PS), formed by a thickening of the caudal portion of the epiblast that extends anteriorly along the embryo midline. Soon after, the PS starts to regress and progressively shortens as gastrulation takes place in the posterior region of the embryo, forming the three embryonic germ layers. This process occurs over time, originating an AP gradient of differentiation concomitantly with embryo elongation (reviewed in Bénazéraf and Pourquié, 2013).

The use of the chick embryo model has been greatly facilitated by detailed developmental staging systems proposed over the years (Stern, 2018; Streit and Stern, 2008). These standardized classification methods facilitate effective communication and comparison of experimental findings between laboratories and remain a cornerstone of chick embryo research and developmental biology as a whole. The Hamburger-Hamilton (HH) staging system, originally published in 1951 (Hamburger, V., & Hamilton, 1951) and republished in 1992 (Hamburger and Hamilton, 1992), is the most commonly used classification to describe chick embryo development. It establishes distinct embryonic stages based on morphological characteristics and encompasses chick development since the laying of the egg until hatching. However, there are limitations to the HH staging system. Namely, it provides insufficient temporal resolution for early developmental stages which lack variety of morphological structures to use as reference. This is the case for HH1, and in 1976 Eyal-Giladi and Kochav provided a detailed classification of the chicken embryo before the formation of the primitive streak, distinguishing between 14 different stages (EGK I–XIV) (Eyal-Giladi and Kochav, 1976), which are all included in stage HH1 (Stern, 2018). Similar difficulties arise in stages HH4 to HH6 (full extension of the PS and early PS regression stages), where visible morphological changes are insufficient for a detailed temporal resolution of the complex cellular and molecular alterations taking place during this developmental period. Also, HH classification largely relies on the quantification of somite pairs during somitogenesis stages (HH7 – HH14), which impedes staging when experiments affect somitogenesis. These gaps highlight the need for additional morphological criteria capable of discriminating developmental time.

Herein, we performed a thorough description of early chicken embryo elongation with high temporal and spatial resolution. To that end, we performed time-lapse imaging of chicken embryos and measured the distances between multiple morphological landmarks over time, from HH4 to HH10. We describe the elongation rates of the embryo anterior-posterior axis as a whole and of several of its composing parts and uncovered a direct proportionality between the length of different embryonic tissues and developmental time. We present a novel morphometric tool made freely accessible to the chick community, termed ChEEQ: Chicken Embryo Elongation Quantification. ChEEQ allows interactive data visualization and can be used to detect and quantify deviations to normal parameters of tissue elongation upon experimental manipulation. Our work provides a time-resolved morphometric dataset using redundant morphological landmarks, that may be used to complement the HH chick embryo staging.

2. Materials and methods

2.1. Chicken embryo culture

Fertilized chicken (*Gallus gallus*) eggs were acquired from commercial sources (Pintobar Exploração Agrícola, Lda, Portugal and Sociedade Agrícola da Quinta da Freiria, S.A., Portugal) and incubated at 38 °C in a humidified atmosphere until the desired developmental stage (Hamburger, V., & Hamilton, 1951). Embryos collected at HH3^{+}- HH6 were cultured using the Easy Culture (EC) (Chapman et al., 2001) (embryos no.1-8, 14–19) or New Culture (New, 1955) (embryos no.9-13, 20) systems, incubated at 38 °C in a humidified atmosphere. For *ex ovo* imaging, a humidified stage-top incubator (UNO-T H-301-k, OKOLAB) or humidified custom-built chamber at 38 °C were used.

2.2. Image acquisition and analysis

Images were captured from the ventral side of the embryo every 3–6 min for a period of up to 27 h, using a Lumar V12 (Zeiss) stereomicroscope coupled with a Zeiss Axiocam Mrc camera. All acquired videos are deposited at Bioimage Archive (Hartley et al., 2022) and can be accessed at DOI: 10.6019/S-BIAD1474.

2.3. Embryo staging and temporal alignment

Embryos were classified according to HH staging system, without the use of + and – subdivisions (Hamburger, V., & Hamilton, 1951; Selleck and Stern, 1991; Streit and Stern, 2008). A new somite pair was considered to be completely formed when both posterior somitic clefts were clearly visible from their axial to lateral limits. Embryos were temporally aligned using the last frame in stage HH4 (time = 0) or the first frame in HH8 (4 somites) as reference.

2.4. Embryo measurements

Tissue length measurements were performed from stage HH4 onwards in selected images (representing 1 h time intervals), using Axiovision Se64 Rel 4.9.1 (Carl Zeiss) or Fiji software (Schindelin et al., 2012). The measurements were performed when landmarks were visible. Namely, C-pPL: anterior-most portion of the embryo to the posterior limit of the *area pellucida* (pPL); C-PS: anterior-most portion of the embryo to the posterior limit of the primitive streak (PS); C-N: anterior-most portion of the embryo to the node; N-PS: node to the posterior limit of the PS; N-pPL: node to the pPL; C-HF: crown to the posterior limit of the head-fold (corresponding to the margin of the anterior intestinal portal); C-Seg: crown to the middle of the second somite; SEG: anterior border of the rostral-most somite to the posterior border of the last formed somite; PSM: posterior border of the last formed somite to the node. N-PS and N-pPL were measured from the first frame at HH5 onwards. A total of 2616 measurements were conducted on 20 different embryos, ranging from stages HH4 to HH10 (Supplementary Table 1).

2.5. Data analysis

Data analysis was performed using R (version 4.4.1) (R Core Team, 2024) in RStudio (Version, 2024.9.0.375) (Posit team, 2024). R packages ggplot2 (version 3.5.1), ggthemes (version 5.1.0), GGally (version 2.2.1), ggridges (version 0.5.6), magrittr (version 2.0.3), viridis (version 0.6.5), dplyr (version 1.1.4), tidyverse (version 2.0.0), tidyr (version 1.3.1), stringr (version 1.5.1), rstatix (version 0.7.2) and purrr (version 1.1.0) were used for data tidying, wrangling, visualization and analysis. Additionally, FactoMineR (version 2.11) and factoextra (version 1.0.7) were used to perform Principal Component Analysis (PCA) and visualize the results. Elongation rate calculations excluded cases where only two length measurements were available. SPSS software was used to apply an Optimal Binning algorithm to optimally discretise the quantitative variables in relation to the categorical variables. To compare outcomes between EC and New culture embryos, we first assessed data normality using the Shapiro-Wilk test. Based on these results, data were analysed with the *t*-test. Statistical tests were performed using data from embryos in stages HH5-HH9 ($n \geq 3$ embryos per culture). To assess the similarity of measurement distributions across developmental stages, pairwise distribution overlaps were computed using a non-parametric kernel density-based approach. For each measurement, the empirical data corresponding to each Hamburger-Hamilton (HH) stage was first summarized by estimating its probability density function using kernel density estimation with Sheather-Jones bandwidth selection. The pairwise overlap between two stages was then quantified by integrating the minimum of their respective density functions across the region where both have support. Formally, for two stages with densities $f_1(x)$ and

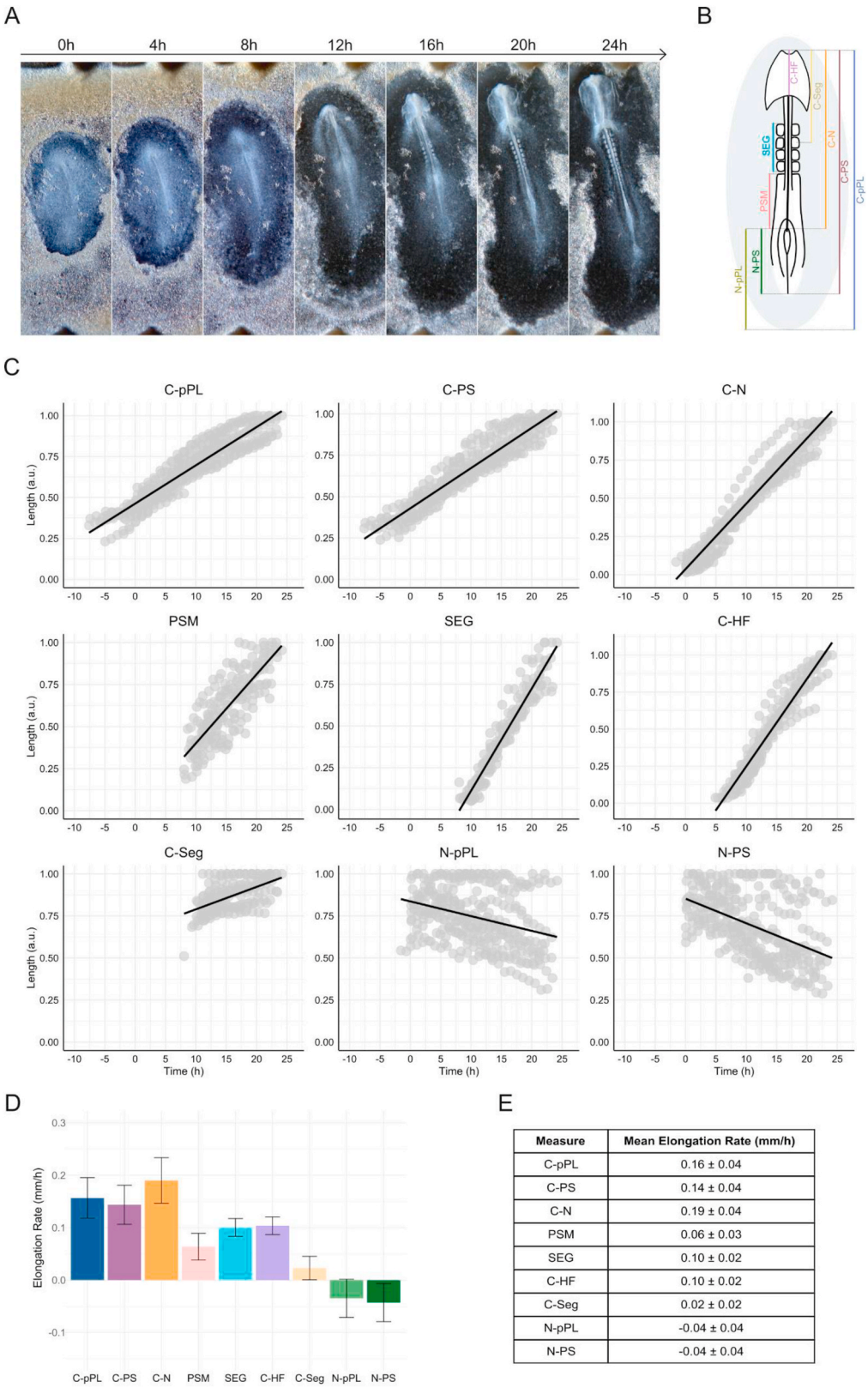

Measure	Mean Elongation Rate (mm/h)
C-pPL	0.16 ± 0.04
C-PS	0.14 ± 0.04
C-N	0.19 ± 0.04
PSM	0.06 ± 0.03
SEG	0.10 ± 0.02
C-HF	0.10 ± 0.02
C-Seg	0.02 ± 0.02
N-pPL	-0.04 ± 0.04
N-PS	-0.04 ± 0.04

Fig. 1. Early chick embryo anterior-posterior elongation over time.
(A) Representative time-lapse images of chicken embryo development. **(B)** Identification of the morphological landmarks used for the measurements performed. **(C)** Normalized length measurements (0–1, arbitrary units) of each tissue over time (h). Linear regression is highlighted. **(D-E)** Elongation rates (mm/h) of each embryo portion analysed. Mean ± standard deviation is shown. C-pPL: anterior-most portion of the embryo to the posterior limit of the *area pellucida* (pPL); C-PS: anterior-most portion of the embryo to the posterior limit of the primitive streak (PS); C–N: anterior-most portion of the embryo to the node; N-PS: node to the posterior end of the PS; N-pPL: node to the pPL; C-HF: crown to the posterior limit of the head-fold; C-Seg: crown to the middle of the second somite; SEG: anterior border of the rostral-most somite to the posterior border of the last formed somite; PSM: posterior border of the last formed somite to the node. Time = 0 corresponds to the transition from HH4 to HH5 in each embryo.

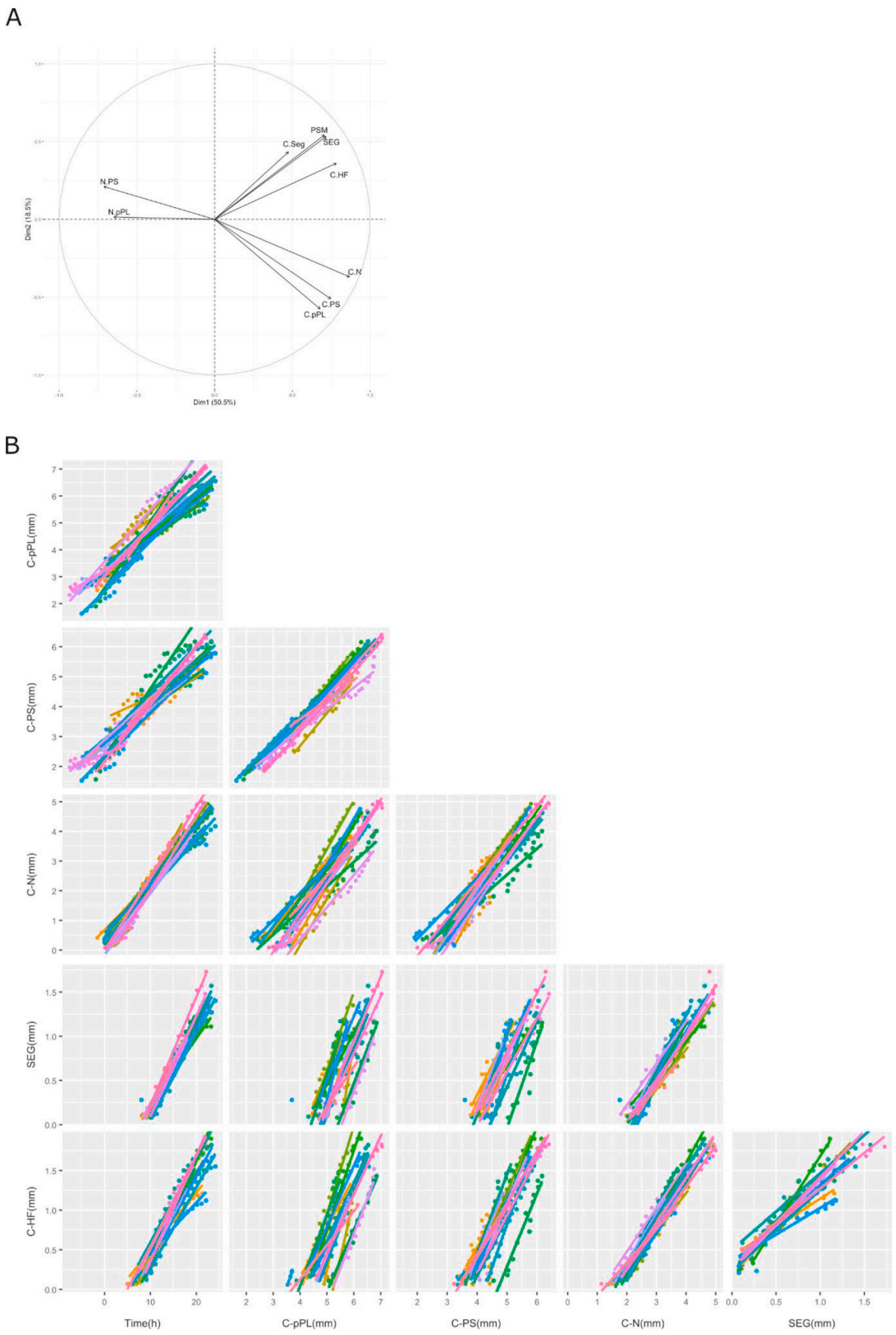

Fig. 2. Correlation between the elongation of multiple tissues and with developmental time.
(A) Principal component analysis of the embryonic measurements performed. **(B)** Pair plot analysis of linear correlations between length measurements and developmental time. C-pPL: anterior-most portion of the embryo to the posterior limit of the *area pellucida* (pPL); C-PS: anterior-most portion of the embryo to the posterior limit of the primitive streak (PS); C–N: anterior-most portion of the embryo to the node; N-PS: node to the posterior end of the PS; N-pPL: node to the pPL; C-HF: crown to the posterior limit of the head-fold; C-Seg: crown to the middle of the second somite; SEG: anterior border of the rostral-most somite to the posterior border of the last formed somite; PSM: posterior border of the last formed somite to the node. Time = 0 corresponds to the transition from HH4 to HH5 in each embryo. Colours represent individual embryos and lines correspond to the linear regression of the data per embryo.

$f_2(x)$, the overlap score is defined as: Overlap $= \int \min(f1(x), f2(x))dx$. This integral captures the shared probability mass between the two distributions. The method yields values bounded between 0 and 1, where 0 indicates complete separation (no overlap) between the distributions, and 1 indicates identical distributions with full overlap. Intermediate values reflect partial overlap, with larger values indicating greater similarity. The overlap calculation was implemented using numerical integration over a common evaluation grid, ensuring consistent comparison across pairs. This approach is advantageous because it makes no distributional assumptions, accounts for differences in spread and shape, and remains robust to sample size variations due to the use of normalized density estimates. It also mirrors well the visual intuition of overlap between the ridge plots of adjacent HH stages. The R code used in all analysis is freely available at the GitHub repository: https://github.com/EmbryoClock/ChickElong.

2.6. ChEEQ: Chicken Embryo Elongation Quantification tool

A Python analysis tool was developed as a notebook in the Google Colab ("Google Colab FAQ," n. d.) environment using Python version 3.10 (Guido Van Rossum, 2009). Colab was chosen for its simplicity and accessibility, offering instant online deployment and ease of use for collaborators. The tool leverages several Python libraries essential for data manipulation and visualization: numpy for numerical operations, pandas for data handling, scipy for statistical computations, and seaborn for plotting. Google Colab Forms interface was utilized to streamline user input, allowing for easy entry of data and analysis parameters directly within the notebook. The full code, reference dataset and example data are available at GitHub: https://github.com/EmbryoClock/ChickElong.

ChEEQ allows for easy user data entry and choice of the analysis parameters. Data input is facilitated by either manual entry or by the upload of a custom Excel spreadsheet into the Colab environment. The tool provides functionality to plot various embryo measurements against each other or over time. Linear regression models are computed, with calculation of confidence intervals around the estimated regression parameters to aid in statistical interpretation. User data can be overlaid on these reference plots, where manually entered or spreadsheet-based data points can be tested against the reference confidence bands to assess statistical significance. The tool also enables comparative analyses over time between different culture conditions and the reference data. All generated plots can be exported as PDF files for documentation and further analysis, ensuring reproducibility and ease of reference for future research. The ChEEQ tool is freely available at https://colab.research.google.com/github/EmbryoClock/ChickElong/blob/main/ChEEQ/ChEEQ.ipynb.

3. Results and discussion

3.1. Characterization of chicken embryo tissue elongation from early gastrulation (HH4) to 10-somite stage (HH10)

To characterize the elongation dynamics of early chicken embryo development, time-lapse imaging of cultured embryos ranging from HH4 to HH10 (Hamburger, V., & Hamilton, 1951) was performed with 3–6 min resolution (N = 20). Morphological landmarks were selected to perform length measurements of multiple portions of the embryo along the anterior-posterior (AP) axis (Fig. 1A and B). The underlying rational was to 1) obtain a quantitative description of embryo elongation and to 2) identify length measurements that can be used to describe developmental time and/or HH embryo stages with some level of redundancy.

The length of the different embryo portions normalized to their maximum value was plotted against time (Fig. 1C; see Supplementary Fig. 1 for absolute length values per embryo) and the average rates of tissue elongation were determined (Fig. 1D and E). The total length of the embryo is represented by C-pPL (measured from the anterior-most portion of the embryo to the posterior limit of the *area pellucida*) and by C-PS (anterior-most portion of the embryo to the posterior limit of the primitive streak) (Fig. 1B and C). The obtained data evidence that the embryo elongates continuously over time, despite major changes in embryo morphology that take place from full length primitive streak stage (HH4) until the formation of 10 somites (HH10). C-pPL and C-PS measurements show similar dynamics with elongation rates of 0.16 ± 0.04 mm/h and 0.14 ± 0.04 mm/h, respectively (Fig. 1D and E). This supports the use of C-pPL as a reliable user-friendly proxy for total embryo length assessment, as previously described (Maia-Fernandes et al., 2019). We found that embryo growth dynamics is independent of the *ex ovo* culture system employed (Supplementary Fig. 2), so all embryos were used in the remaining analysis, irrespective if incubated in New or EC cultures.

In early embryonic stages, elongation occurs concomitantly with node regression and notochord elongation along the AP axis. This is depicted by the C-N measurement, which also shows a linear growth (Fig. 1C–C-N), with an elongation rate of 0.19 ± 0.04 mm/h (Fig. 1D and E). Concomitantly, the primitive streak gradually shortens (N-PS: −0.04 ± 0.04 mm/h), as does the distance between the node and the posterior limit of the *area pellucida* (N-pPL: −0.04 ± 0.04 mm/h). This is consistent with gastrulation taking place at the posterior-most region of the embryo, with progressive depletion of epiblast-like cells and shortening of the PS (Spratt, 1947). The application of principal component analysis (PCA) to our data further evidenced the opposing dynamics of the C-PS, C-pPL and C-N measurements with that of N-PS and N-pPL (Fig. 2A). In fact, these are positioned in opposite quadrants of the PCA.

A third PCA cluster, positioned roughly perpendicular to the former two, contains the remaining measurements performed, namely C-Seg, SEG, PSM and C-HF (Fig. 2A). The lengths of the presomitic mesoderm (PSM) and of the segmented region of the trunk (SEG) increase over time, at a rate of 0.06 ± 0.03 mm/h and 0.10 ± 0.02 mm/h, respectively (Fig. 1C–E and Supplementary Fig. 1). The SEG region increases as new somites are being formed from the rostral-most portion of the PSM; hence, the observed elongation of the PSM indicates that the rate of PSM shortening due to somite formation is largely compensated by other elongation mechanisms operating in this tissue. These include a high volumetric expansion and proliferation speed, significantly contributing to chick embryo axial elongation (Bénazéraf et al., 2017). While the C-Seg measure is not significantly altered as development proceeds (Fig. 1C–E) (C-Seg: 0.02 ± 0.02 mm/h), the head-fold (C-HF) grows significantly in a parallel embryonic plane. In fact, its rate is strikingly similar to that of the segmented region (SEG), also elongating at a rate of 0.10 ± 0.02 mm/h (Fig. 1C–E).

Of the measurements performed, C-pPL, C-PS, C-N, SEG and C-HF vary linearly with time (Fig. 2B, Supplementary Fig. 3). From these, C-N, SEG and C-HF show less inter-embryo variability, making them suitable candidates as proxy for developmental time, i.e., one can reliably infer time (h) from length (mm). This may allow, for example, the temporal alignment of independent embryos using length measurements alone, or the comparison between the rate of embryo development in different experimental conditions. C-PS and C-pPL are further correlated with C-N and SEG (Fig. 2B). Unexpectedly, our data also unveiled a direct proportionality between C-HF and both C-PS and C-pPL. Hence, measuring the distance from the embryo crown to the posterior limit of the head-fold (C-HF) can be used to infer the total length of the embryo at any given time. C-HF is further capable of describing C-N and SEG, despite elongating in a parallel plane to the main embryonic axis. Unveiling these correlations can be very useful in experimental conditions when a specific tissue is manipulated, and an internal control is required to detect and quantify deviations to normal elongation. For example, C-HF length may be used as a reliable proxy for SEG length, in experiments where somite formation is experimentally challenged without perturbing C-HF development.

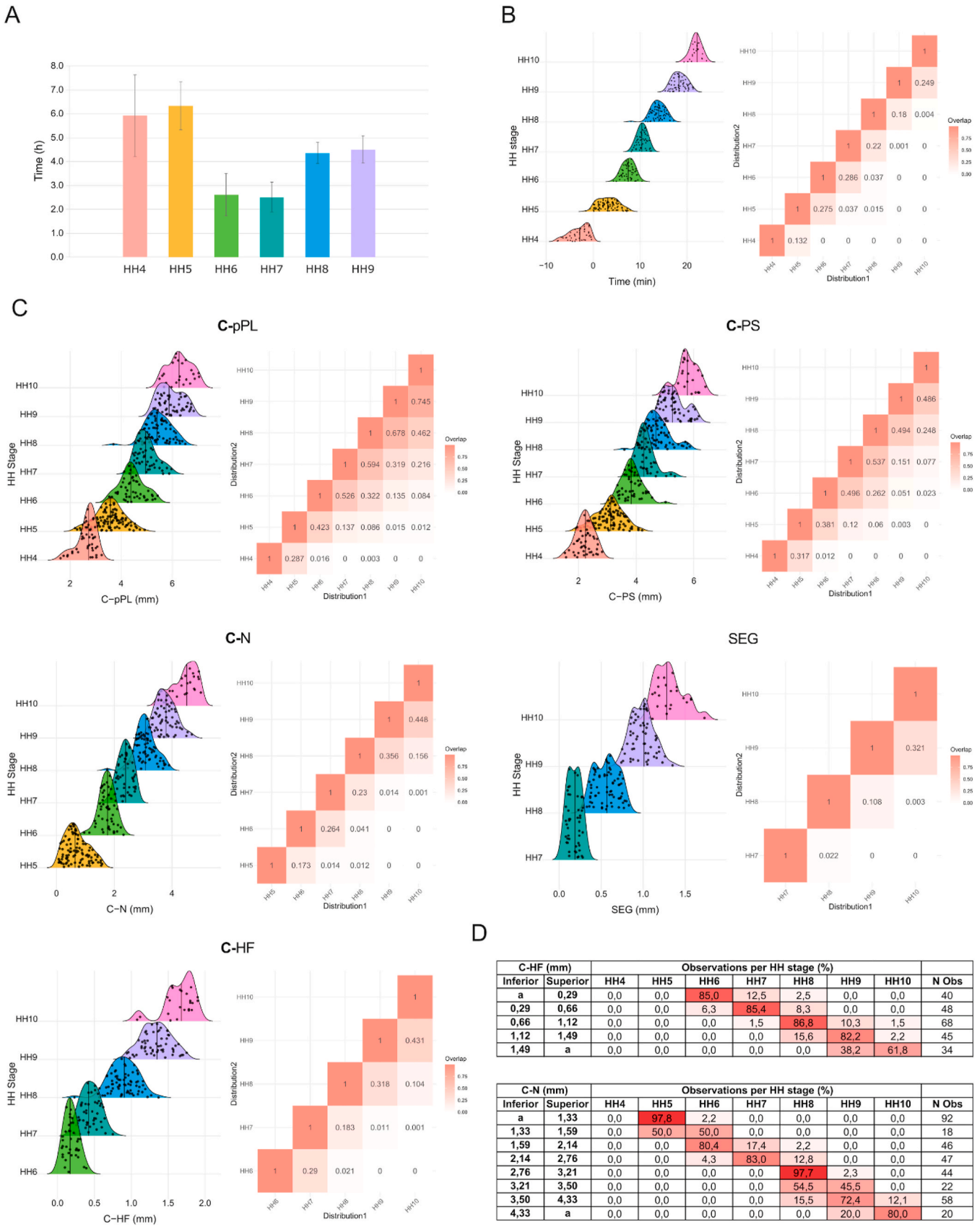

D

C-HF (mm)		Observations per HH stage (%)							
Inferior	Superior	HH4	HH5	HH6	HH7	HH8	HH9	HH10	N Obs
a	0,29	0,0	0,0	85,0	12,5	2,5	0,0	0,0	40
0,29	0,66	0,0	0,0	6,3	85,4	8,3	0,0	0,0	48
0,66	1,12	0,0	0,0	0,0	1,5	86,8	10,3	1,5	68
1,12	1,49	0,0	0,0	0,0	0,0	15,6	82,2	2,2	45
1,49	a	0,0	0,0	0,0	0,0	0,0	38,2	61,8	34

C-N (mm)		Observations per HH stage (%)							
Inferior	Superior	HH4	HH5	HH6	HH7	HH8	HH9	HH10	N Obs
a	1,33	0,0	97,8	2,2	0,0	0,0	0,0	0,0	92
1,33	1,59	0,0	50,0	50,0	0,0	0,0	0,0	0,0	18
1,59	2,14	0,0	0,0	80,4	17,4	2,2	0,0	0,0	46
2,14	2,76	0,0	0,0	4,3	83,0	12,8	0,0	0,0	47
2,76	3,21	0,0	0,0	0,0	0,0	97,7	2,3	0,0	44
3,21	3,50	0,0	0,0	0,0	0,0	54,5	45,5	0,0	22
3,50	4,33	0,0	0,0	0,0	0,0	15,5	72,4	12,1	58
4,33	a	0,0	0,0	0,0	0,0	0,0	20,0	80,0	20

(caption on next page)

Fig. 3. Characterization of Hamburger and Hamilton stages using length measurements.
(A) Average duration of developmental stages HH4 to HH9, determined from time-lapse imaging data. **(B)** Temporal distribution of the HH classification for all measured frames: ridge plot visualization and pairwise overlap matrix (left and right, respectively). **(C)** Ridge plot of the length measurements of each embryo portion per HH stage and corresponding overlap matrix (left and right, respectively). (D) HH stage discrimination based on C-HF and C-N measurements defined by an optimal binning algorithm. Specific length intervals (or bins) are identified that best reflect the probability of an embryo being assigned to a particular HH stage. "Inferior" indicates the lower boundary of a length interval, while "Superior" denotes its upper boundary. C-pPL: anterior-most portion of the embryo to the posterior limit of the *area pellucida* (pPL); C-PS: anterior-most portion of the embryo to the posterior limit of the primitive streak (PS); C–N: anterior-most portion of the embryo to the node; C-HF: crown to the posterior limit of the head-fold; SEG: anterior border of the rostral-most somite to the posterior border of the last formed somite; Time = 0 corresponds to the transition from HH4 to HH5 in each embryo. HH: Hamburger and Hamilton (Hamburger, V., & Hamilton, 1951).

3.2. Spatio-temporal description of Hamburger and Hamilton (HH) stages of development

To determine the mean duration of each developmental stage, all acquired images per embryo were classified according to HH (Hamburger, V., & Hamilton, 1951), and the time difference between the first frame of two consecutive HH stages was determined (Fig. 3A). HH4 and HH5 encompass several hours of development (HH4: 5.9 ± 1.7 h; HH5: 6.3 ± 1.0 h), without the formation of morphological structures capable of discriminating early-vs late-HH4/5 stages with precision (Fig. 3A and B). HH6 and HH7 have a significantly shorter duration (HH6: 2.6 ± 0.9 h; HH7: 2.5 ± 0.6 h). This is in line with the previously described transitory nature of HH6, and in HH7 only two somite pairs are formed (Hamburger, V., & Hamilton, 1951). The average duration of the remaining early somitogenesis stages (HH8: 4.4 ± 0.4 h; HH9: 4.5 ± 0.6 h) (Fig. 3A and B) is consistent with the formation of three new somite pairs from each stage to the next, as these take 75–90 min to form each (Maia-Fernandes et al., 2024). Temporal overlap of HH stages (Fig. 3B) reflects embryo-to-embryo stage duration variability as previously described (Hamburger, V., & Hamilton, 1951).

Plotting the measurements of each embryonic portion against the corresponding HH stage (Fig. 3C) shows that total embryo elongation (C-pPL and C-PS) mirrors HH progression over time (Fig. 3B). Three other embryo portions, C-N, SEG and C-HF also elongate as HH stages progress (Fig. 3C). Hence, these measures have the potential to discriminate between HH stages of development, albeit with some degree of overlap, as reflected by pairwise overlap matrix analysis (right panels per embryo portion). On the contrary, N-pPL, N-PS, C-Seg and PSM, show the highest overlap between different HH stages (Supplementary Fig. 4).

Somite number is key for HH classification in early somitogenesis (Hamburger, V., & Hamilton, 1951). Since our aim was to identify a putative redundant proxy for HH, we interrogated the ability of C-N or C-HF to discriminate HH stages of development. C-HF is particularly interesting for this purpose because this tissue develops in a parallel plane to the embryo body axis. For that, we applied an optimal binning algorithm to the C-HF and C-N data to obtain discrete length intervals which are indicative of the likelihood of the embryo to pertain to a specific HH stage. Indeed, C-HF and C-N length intervals revealed high HH predictive power (Fig. 3D). For example, 97.7 % of embryos with C-N measuring 2.76 mm–3.21 mm (inferior and superior limits, respectively) are in the HH8 developmental stage. Some length intervals, however, have limited discriminatory power. For example, embryos with C-N measuring 3.21 mm–3.50 mm may belong to HH8 (54.5 %) or HH9 (45.5 %), which correspond to embryos in significantly different developmental time points.

Overall, we show tissue specific length measurements provide a new quantitative layer of information to HH stages of development. This allows the classification of HH stages using alternative morphological landmarks. To temporally order different embryos belonging to the same HH stage, however, requires a greater level of temporal resolution, which may be provided by time-lapse imaging analysis.

3.3. ChEEQ: a novel morphometric tool for the analysis of chick embryo elongation dynamics

The currently available experimental technologies, which include the ability to perform imaging of the same embryo over time, provide important information that may aid in the comprehension of scientific questions that require great temporal resolution. Using the new dataset of early chick embryo measurements acquired over time, we developed an open-source computational tool termed **ChEEQ** - **Ch**icken **E**mbryo **E**longation **Q**uantification - with the purpose of making our data readily accessible for visualization and interaction to the scientific community, complying with FAIR data principles (Wilkinson et al., 2016). ChEEQ includes a total of 2616 data entries, concerning 9 different measurements (Fig. 1B) performed on 20 embryos at 1-h intervals, for up to 27 h of incubation (a total of 390 measured images). The ChEEQ tool allows 1) the visualization and exploration of the dataset herein described, as well as 2) the analysis of the user's own experimental data (static images or time-lapse imaging) in comparison with the reference dataset provided. ChEEQ is applicable to embryos from HH4 to HH10, and the usage of specific measurements depends on the developmental stage (for example, C-HF can only be used from HH6 onwards, when the head-fold is first identified).

Upon initializing the program, the ChEEQ user is presented with multiple options for graphical visualization and analysis of the original dataset (Fig. 4A). These include the representation of all, or individual measurements (in the yy axis) plotted against time or one of the time-proxy lengths identified in this work, namely, C-N or C-HF (xx axis). Measurements can be visualized as absolute values or relative to total embryo length measurements (C-pPL and C-PS), to SEG, or to C-HF. Data can be discriminated per embryo and linear regression analysis can be performed with user-selected confidence intervals (Fig. 4A). Residual plot visualization is also available.

An important functionality of ChEEQ is the ability to analyse new experimental data by contrasting it to the reference dataset (Fig. 4B and C). Measurements performed in a single time point, i.e. one image (Fig. 4B) or over a period of time (Fig. 4C), can be uploaded from a file or inserted manually, and compared to the reference dataset as long as the same morphological landmarks are used for length measurements. Alignment for comparison of these new data with the reference dataset is performed using C-N or C-HF as a proxy for time. Deviations to the reference can, thus, be interpreted as time displacements, i.e., if an experimental manipulation results in shortening of the C-N region of the embryo, one can estimate how much time this tissue is delayed in development in comparison with the wildtype conditions (Fig. 4B). Also, comparison of the linear regression parameters between new time-lapse measurements and the reference dataset can quantify alterations to embryo elongation dynamics, for example (Fig. 4C).

The information provided by the ChEEQ tool, including the linear regression analysis between different measurements, allows the user to identify which tissues may be used as reference for time progression, depending on the type of experimental manipulation being performed. We anticipate this can be especially useful when the PSM or the SEG region are perturbed. The chicken embryo is a long-standing model system in the study of vertebrate segmentation (Pourquié, 2004) and during early somitogenesis, the number of somites is used for HH embryo staging (Hamburger, V., & Hamilton, 1951). Our tool thus provides

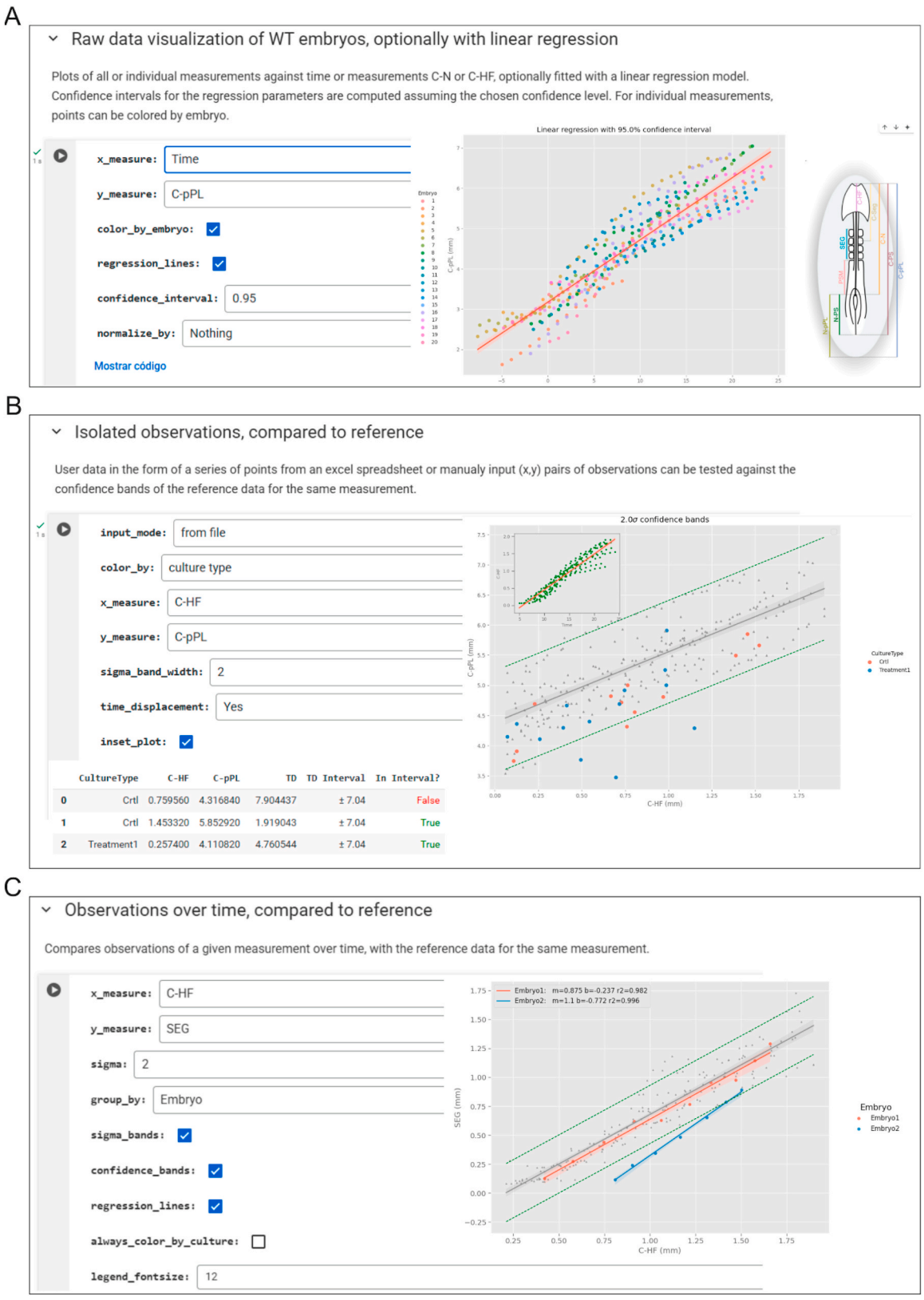

Fig. 4. ChEEQ - Chicken Embryo Elongation Quantification tool for interactive data visualization and analysis.
(A) The ChEEQ tool allows a straightforward visualization of the reference chick embryo length measurements herein described, providing multiple options for graphical representation. The example plot shown is of C-pPL against time, with data coloured per embryo and a linear regression model. **(B, C)** ChEEQ allows to compare user-input experimental data with the reference dataset using **(B)** single time-point measurements or **(C)** measurements performed over time. Alignment with reference data is accomplished using C-N or C-HF as proxy for time. When deviations are observed (B), the distance to the mean is quantified as temporal displacement (TD).

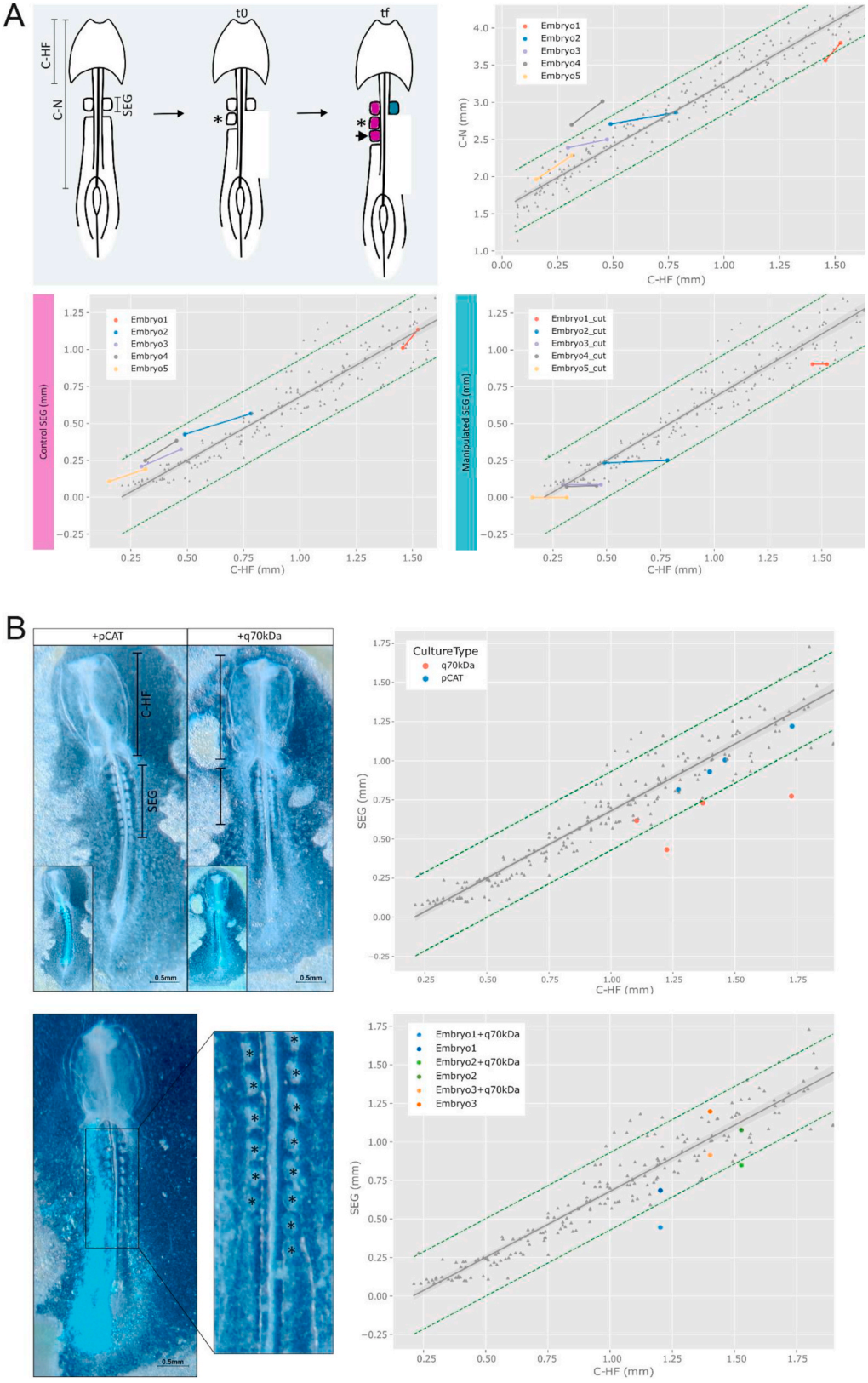

Fig. 5. C-HF is a reliable proxy for developmental time upon perturbation to somite formation. **(A)** ChEEQ tool was applied to embryos where the presomitic mesoderm was ablated on one side, and development progressed until the formation of a new somite on the control side (as in Maia-Fernandes et al., 2024). **(B)** Application of the ChEEQ tool to embryos where somite segmentation was inhibited by overexpression of the 70 kDa fibronectin matrix inhibitor on both sides of the presomitic mesoderm (PSM) (as in de Almeida et al., 2022) (upper panel) or only on one side (lower panel). In (A) asterisks and arrowheads mark the last formed somite at the moment of PSM ablation (t0) and when a new somite is formed (tf), respectively. Asterisks in (B) represent somites formed.

an alternative way to temporally align different embryos - even when somite formation is perturbed - by employing other morphological measurements as proxy for developmental time. To exemplify this, ChEEQ was used to quantify alterations to tissue elongation in experimental conditions involving presomitic mesoderm manipulation and consequent perturbation of somite formation, reported in previous work from our lab (Maia-Fernandes et al., 2024; de Almeida et al., 2022) (Fig. 5A and B, respectively). Fig. 5A shows that upon ablation of the PSM tissue on one side of the embryo (as performed in Maia-Fernandes et al., 2024), C-N and C-HF were not significantly affected, as they elongated along with somite formation on the contralateral control side (see also Supplementary Fig. 5). Fig. 5B presents experiments where somite formation was impaired by over-expression of a dominant-negative inhibitor of fibronectin matrix assembly, the 70 kDa fragment (as in de Almeida et al., 2022). The upper panel (Fig. 5B) shows that bilateral perturbation to somite formation is detected by ChEEQ, since shorter SEG regions are observed in the experimental embryos (q70kDa) compared to the controls (pCAT), while C-HF measures are within the same range. Perturbing somite formation only on one side of the embryo (Fig. 5B, bottom panel) did not alter C-HF elongation, as it maintains its proportion to the control side. Together, these examples evidence that C-HF elongation is robust to perturbations to the PSM or somite formation, and that it can be used to describe developmental time when somite number is not a reliable staging metric.

4. Conclusions

In this work, we report a detailed morphometric characterization of chick embryo elongation from HH4 to HH10. This approach generated two freely accessible resources for the chick community. Namely, a time-lapse image dataset comprising a total of 20 embryos cultured *ex ovo* for up to 27 h (images acquired every 3–6 min), and a new dataset of embryo length measurements over time. We identified embryo length measurements that elongate in a linear fashion over time from HH4-HH10, such as the total embryo length (C-pPL and C-PS), as anticipated. Interestingly, the head-fold (C-HF) also showed a strong correlation with time although it elongates above the main embryonic axis. These finding enables the temporal alignment of independent embryos using length measurements alone. This is particularly relevant because it is not possible to attribute an absolute developmental time to chicken embryos, since their development initiates before the egg is laid. Additionally, we provide a morphometric characterization of HH stages and report a new computational tool available to the chick embryo community – ChEEQ – which allows the analysis of the effect of experimental manipulations on embryo tissue elongation, by direct comparison with our new reference dataset. These new resources may be leveraged to answer lingering questions on vertebrate embryo elongation, as well as quantitatively address the impact of different embryo manipulations on overall development.

CRediT authorship contribution statement

A.C. Maia-Fernandes: Writing – review & editing, Writing – original draft, Visualization, Validation, Methodology, Investigation, Formal analysis, Conceptualization. **T. Pais de Azevedo:** Visualization, Methodology, Investigation, Formal analysis. **N. Borralho-Martins:** Writing – review & editing, Methodology, Investigation, Formal analysis. **S. Ramalhete:** Visualization, Methodology, Formal analysis, Data curation. **G.G. Martins:** Supervision, Methodology, Investigation. **I. Palmeirim:** Supervision, Investigation. **I. Duarte:** Visualization, Formal analysis, Data curation, Conceptualization. **A. Marreiros:** Supervision, Methodology, Formal analysis, Conceptualization. **P.J. Martel:** Visualization, Software, Methodology, Formal analysis. **R.P. Andrade:** Writing – review & editing, Writing – original draft, Visualization, Supervision, Resources, Methodology, Investigation, Funding acquisition, Conceptualization.

Funding information

This work was supported by Fundação para a Ciência e Tecnologia, SFRH/BD/146043/2019 (10.54499/SFRH/BD/146043/2019) and COVID/BD/153553/2024 to ACMF, 2022.12867.BD (10.54499/2022.12867.BD) to NBM, 2021.00238.CEECIND and RISE - LA/P/0053/2020 to ID, and by AD-ABC to RPA and TPA.

Acknowledgements

The authors thank I. T. Afonso for inspiring the tool acronym. We also acknowledge the support provided by the Microscopy Unit of ABC-RI, Portuguese Platform for Bioimaging (reference PPBI-POCI-01-0145-FEDER-022122).

Appendix A. Supplementary data

Supplementary data to this article can be found online at https://doi.org/10.1016/j.ydbio.2025.12.022.

Data availability

All data and code are freely accessible, as described in the manuscript file

References

Bénazéraf, B., Beaupeux, M., Tchernookov, M., Wallingford, A., Salisbury, T., Shirtz, Amelia, Shirtz, Andrew, Huss, D., Pourquié, O., François, P., Lansford, R., 2017. Multi-scale quantification of tissue behavior during amniote embryo axis elongation. Dev 144, 4462–4472. https://doi.org/10.1242/dev.150557.

Bénazéraf, B., Pourquié, O., 2013. Formation and segmentation of the vertebrate body axis. Annu. Rev. Cell Dev. Biol. 29, 1–26. https://doi.org/10.1146/annurev-cellbio-101011-155703.

Chapman, S.C., Collignon, J., Schoenwolf, G.C., Lumsden, A., 2001. Improved method for chick whole-embryo culture using a filter paper carrier. Dev. Dyn. 220, 284–289. https://doi.org/10.1002/1097-0177(20010301)220:3<284::AID-DVDY1102>3.0.CO;2-5.

de Almeida, P.G., Rifes, P., Martins-Jesus, A.P., Pinheiro, G.G., Andrade, R.P., Thorsteinsdóttir, S., 2022. Cell-Fibronectin interactions and actomyosin contractility regulate the segmentation clock and spatio-temporal somite cleft Formation during chick embryo somitogenesis. Cells 11. https://doi.org/10.3390/CELLS11132003.

Eyal-Giladi, H., Kochav, S., 1976. From cleavage to primitive streak formation: a complementary normal table and a new look at the first stages of the development of the chick. I. General morphology. Dev. Biol. 49, 321–337. https://doi.org/10.1016/0012-1606(76)90178-0.

Google Colab FAQ Google Colab FAQ [WWW Document], n.d. URL https://research.google.com/colaboratory/faq.html (accessed 10.24.24).

Guido Van Rossum, F.L.D., 2009. Python 3 Reference Manual. CreateSpace Independent Publishing Platform, Scotts Valley, CA.

Hamburger, V., Hamilton, H.L., 1951. A series of normal stages in the development of the chick embryo. J. Morphol. 88, 49–92.

Hamburger, V., Hamilton, H.L., 1992. A series of normal stages in the development of the chick embryo. 1951. Dev. Dyn. 195, 231–272.

Hartley, M., Kleywegt, G.J., Patwardhan, A., Sarkans, U., Swedlow, J.R., Brazma, A., 2022. The BioImage archive – building a home for life-sciences microscopy data. J. Mol. Biol. 434, 167505. https://doi.org/10.1016/J.JMB.2022.167505.

Maia-Fernandes, A., Pais de Azevedo, T., Marreiros, A., Palmeirim, I., Andrade, R., 2019. The posterior limit of the area pellucida (pPL) as a reliable proxy for the end of the primitive streak in chick elongation studies. Matters 1–5. https://access.portico.org/stable?au=pjbm090c.

Maia-Fernandes, A.C., Martins-Jesus, A., Borralho-Martins, N., Pais-De-Azevedo, T., Magno, R., Duarte, I., Andrade, R.P., 2024. Spatio-temporal dynamics of early somite segmentation in the chicken embryo. PLoS One 19, e0297853. https://doi.org/10.1371/JOURNAL.PONE.0297853.

New, D.A.T., 1955. A new technique for the cultivation of the chick embryo in vitro. J. Embryol. exp. Morph. 3, 320–331.

Posit team, 2024. Rstudio: Integrated Development Environment for R. Posit Software. PBC, Boston, MA. http://www.posit.co.

Pourquié, O., 2004. The chick embryo: a leading model in somitogenesis studies. Mech. Dev. 121, 1069–1079. https://doi.org/10.1016/j.mod.2004.05.002.

R Core Team, 2024. R: a Language and Environment for Statistical Computing. R Foundation for Statistical Computing, Vienna, Austria. https://www.r-project.org.

Schindelin, J., Arganda-Carreras, I., Frise, E., Kaynig, V., Longair, M., Pietzsch, T., Preibisch, S., Rueden, C., Saalfeld, S., Schmid, B., Tinevez, J.Y., White, D.J.,

Hartenstein, V., Eliceiri, K., Tomancak, P., Cardona, A., 2012. Fiji: an open-source platform for biological-image analysis. Nat. Methods 2012 97 (9), 676–682. https://doi.org/10.1038/nmeth.2019.

Selleck, M.A.J., Stern, C.D., 1991. Fate mapping and cell lineage analysis of Hensen's node in the chick embryo. Development 112, 615–626. https://doi.org/10.1242/dev.112.2.615.

Spratt, N.T., 1947. Regression and shortening of the primitive streak in the explanted chick blastoderm. J. Exp. Zool. 104, 69–100. https://doi.org/10.1002/JEZ.1401040105.

Stern, 2018. Staging tables for avian embryos: a little history. Int. J. Dev. Biol. 62, 43–48. https://doi.org/10.1387/IJDB.170299CS.

Stern, 2005. The chick: a great model System becomes Even greater. Dev. Cell 8, 9–17. https://doi.org/10.1016/J.DEVCEL.2004.11.018.

Streit, A., Stern, C.D., 2008. Chapter 1 operations on primitive streak stage avian embryos. Methods Cell Biol. 87, 3–17. https://doi.org/10.1016/S0091-679X(08)00201-X.

Wilkinson, M.D., Dumontier, M., Aalbersberg, IjJ., Appleton, G., Axton, M., Baak, A., Blomberg, N., Boiten, J.W., da Silva Santos, L.B., Bourne, P.E., Bouwman, J., Brookes, A.J., Clark, T., Crosas, M., Dillo, I., Dumon, O., Edmunds, S., Evelo, C.T., Finkers, R., Gonzalez-Beltran, A., Gray, A.J.G., Groth, P., Goble, C., Grethe, J.S., Heringa, J., t Hoen, P.A.C., Hooft, R., Kuhn, T., Kok, R., Kok, J., Lusher, S.J., Martone, M.E., Mons, A., Packer, A.L., Persson, B., Rocca-Serra, P., Roos, M., van Schaik, R., Sansone, S.A., Schultes, E., Sengstag, T., Slater, T., Strawn, G., Swertz, M. A., Thompson, M., Van Der Lei, J., Van Mulligen, E., Velterop, J., Waagmeester, A., Wittenburg, P., Wolstencroft, K., Zhao, J., Mons, B., 2016. The FAIR Guiding Principles for scientific data management and stewardship. Sci. Data 2016 31 (3), 1–9. https://doi.org/10.1038/sdata.2016.18.